FIREBALL : Instrument pointing and aspect reconstruction

Mateusz Matuszewski[a], Jean Evrard[b], Frederi Mirc[b], Robert Grange[c], Stephan Frank[c], Bruno Milliard[c], Sarah E. Tuttle[d], Shahinur Rahman[a], D. Christopher Martin[a], David Schiminovich[d], Ryan McLean[a] and Robert G. Chave[e]

[a]Caltech, Cahill Center for Astrophysics, 1216 E California Blvd., Pasadena, CA 91125, USA;
[b]Centre National d'Études Spatiales, 31401 Toulouse CEDEX 4, France;
[c]Laboratoire d'Astrophysique de Marseille, 13388 Marseille CEDEX 13, France;
[d]Columbia University Astronomy Department, 550 W. 120th St., New York, NY 10027, USA;
[e]Robert Chave Applied Physics Inc., P.O. Box 266, Altadena, CA 91003, USA

ABSTRACT

The Faint Intergalactic Redshifted Emission Balloon (FIREBALL) had its first scientific flight in June 2009. The instrument is a 1 meter class balloon-borne telescope equipped with a vacuum-ultraviolet integral field spectrograph intended to detect emission from the inter-galactic medium at redshifts $0.3 < z < 1.0$. The scientific goals and the challenging environment place strict constraints on the pointing and tracking systems of the gondola. In this manuscript we briefly review our pointing requirements, discuss the methods and solutions used to meet those requirements, and present the aspect reconstruction results from the first successful scientific flight.

Keywords: Cosmology, Integral field spectroscopy, FIREBALL, Data reduction, Pointing stabilization

1. POINTING REQUIREMENTS AND ENVIRONMENT

FIREBALL was designed to detect diffuse emission around galaxies, and along cosmic web sheets and filaments that models of structure formation indicate permeate the universe.[1,2] The instrument exploits a small throughput window in the electromagnetic spectrum around 2100Å where the O_2 and O_3 absorption cross sections decrease. FIREBALL is a 4000lb modified prime-focus 1 m alt-azimuth optical telescope equipped with an integral field spectrograph (IFS) and launched on balloon to an altitude of 115,000 feet. It is controlled remotely from the ground via line-of-sight telemetry and uses several transmitters to beam back science and housekeeping data to the control center. The payload experiences temperature, pressure and altitude changes, strong, often shearing, winds, and ballast drops. These effects on the motion of the gondola have to be counteracted to allow for the telescope to perform the task of pointing at fixed targets for extended periods of time.

The FIREBALL field of view consists of a hexagonally packed bundle of 280 fibers. Each of these has a diameter of about 8" on the sky, and the full bundle is $\sim$ 140" across. The typical sizes of the emission regions that FIREBALL targets are on the order of 30-100". The telescope must be held steady to better than 30" to make sure that the target region is within the field of view. Accurate point source and background masking or subtraction requires that the locations of these sources be known well, at the sub-fiber level. This further restricts the pointing requirement to about 1/2 a fiber, or 4" on the sky. FIREBALL makes use of photon-counting microchannel plate (MCP) technology. This relaxes the pointing requirement somewhat, shifting the emphasis on the post-flight aspect solution reconstruction. However, as we anticipate using higher QE CCD detectors for this project in the future, which will operate with longer integration times during which the telescope will have to be kept steady, we retain the 1/2 fiber pointing requirement.

FIREBALL's mission and general design are discussed in Martin et al.[3] in this volume. The details of the integral field spectrograph (IFS) design are given in Tuttle et al.[4] Information about some aspects of data acquisition and processing can be found in Rahman et al.[5]

Further author information:
M.M.: matmat@caltech.edu, Tel: (626) 395 1879

Space Telescopes and Instrumentation 2010: Ultraviolet to Gamma Ray,
edited by Monique Arnaud, Stephen S. Murray, Tadayuki Takahashi, Proc. of SPIE Vol. 7732,
773229 · © 2010 SPIE · CCC code: 0277-786X/10/$18 · doi: 10.1117/12.857869

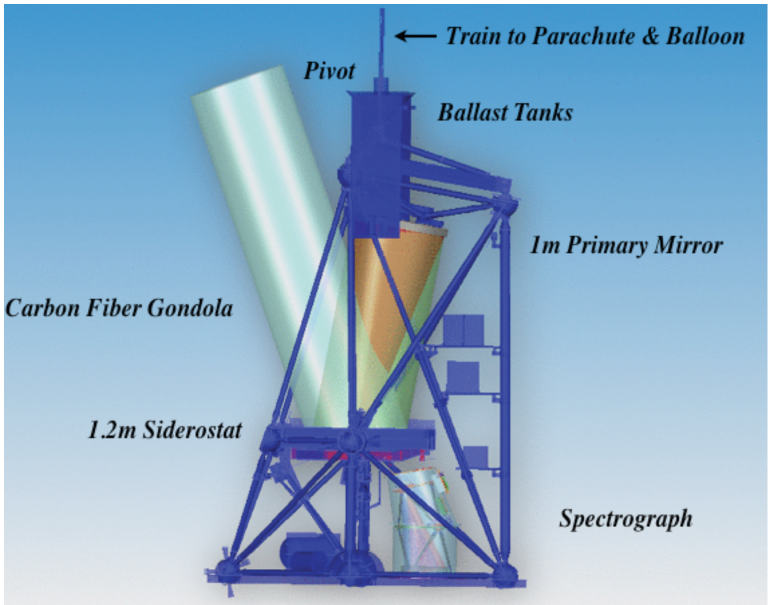

Figure 1. A schematic side view of the FIREBALL gondola. Pointing is accomplished by selecting the target azimuth with the pivot and setting the elevation with the siderostat flat mirror. This mirror reflects the beam onto a stationary 1m F/2.5 parabolic primary, which focuses the light at the instrument focal plane. Before the focal plane, the visible light component is separated from the UV science beam via a high efficiency dichroic and sent to the guider camera.

2. POINTING AND STABILIZATION

The pointing and stabilization of the FIREBALL telescope is accomplished by way of two actuated elements. The gondola pivot has an unlimited range of rotation, allowing for pointing at arbitrary azimuth. The siderostat mirror is mounted on a gimbal frame that allows the tilt angle of the optic to be set so as to observe at any elevation in the range of 40° to 70°, the upper cut-off due to vignetting by the balloon. This mirror also has a cross-elevation tip mechanism that can rotate it in the range ±2° from the nominal orientation. Figure 1 shows a schematic view of the gondola. The two motions of the siderostat are controlled by the fine stabilization control, which makes use of a pre-compensating open loop, and a compensating closed loop. This FIREBALL pointing system solution is based on the those used by the CNES members of the collaboration on the FOCA[6] and PRONAOS[7] gondolas. The pivot and siderostat motors are heritage hardware from those projects. The control instrumentation and algorithms are described in more detail in Huguenin.[8]

Telescope pointing and stabilization is a multi-step process. The initial pointing solution is arrived at by combining the gondola GPS location information with magnetometer orientation data and the desired observation target coordinates. The pivot and siderostat are adjusted to the appropriate azimuth and altitude settings. The boresight is thus kept pointed at the scientific target with an accuracy of a few dozen arcminutes, enough to hold the field within the field of view of an optical target recognition camera. Once the initial pointing solution is acquired, the pointing is refined via through stabilization of each of the two axes by way of a two stage process, each being controlled by one of a pair of computers with the help of an analog signal-mixing tracker card. The first stage, called precompensation, is an open loop control of the siderostat velocity, correcting the telescope boresight for 95% of the gondola's rotation velocity. The second stage is a closed loop control using error signals from an optical monitor. This corrects the residual errors from the precompensation, leaving a nominal RMS guidance error of 3 arcseconds on each axis. The computers responsible for these control loops collect and combine information from a battery of sensors: three gyroscopes that gauge the motion of the gondola for the precompensation, two optical cameras that measure guidance offsets for the closed loops, and a series of housekeeping devices used for various purposes, like an inclinometer and a potentiometer that measure the siderostat's orientation with respect to the gondola. The gains and phases of these signals are adjusted on the

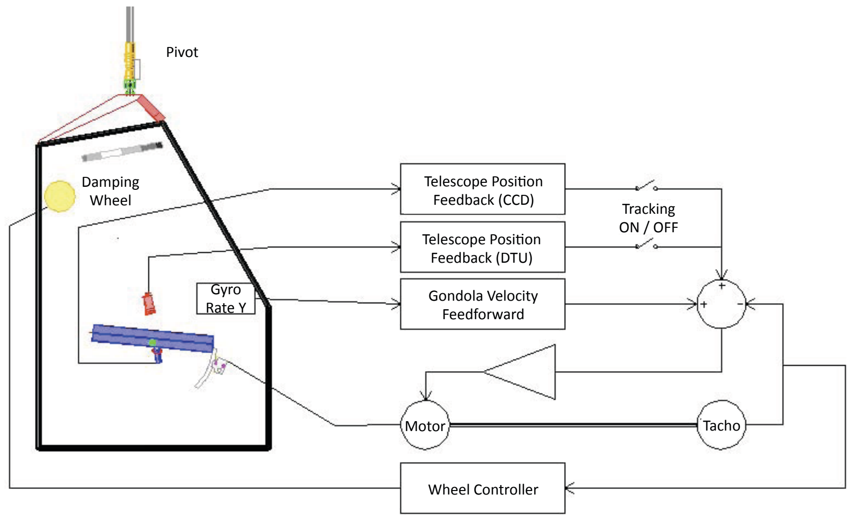

Figure 2. A simplified schematic view of one of the two guidance control loops acting on the siderostat. The rotation of the gondola is measured by a gyroscope attached to the gondola structure, and that velocity information is sent with a 50% angular gain as an open loop signal to the siderostat to precompensate for the line of sight changes due to gondola rotation. That information is then combined with the measured pointing angular errors from one of the guidance cameras, closing the error signal loop. The camera signal is injected with low gain and trims the velocity of the siderosat mirror computed from the precompensation. Such a two stage guidance solution is more stable than conventional guidance with no precompensation. A similar type of two stage stabilization is used for the gondola pivot, which uses the gondola azimuth errors from the magnetometer as input for the closed loop stage, in place of an optical pointing error.

ground with a fully assembled, though lacking the ballast, gondola. There are two optical guidance sensors on-board FIREBALL. The first is a DTU ASC star-tracker camera.[9] This has a large 13.4×18.4 square degree field of view and supplies a corrective signal at 2Hz. Adding this signal into the loops stabilizes the pointing to about 1 arcminute, which brings the target region into the field of view of the second sensor, the dedicated optical guider. This is a camera that was built specifically for the FIREBALL mission; some of the details of its operation are described in the next section. This optical guider has a field of view of 28'×24' that contains the location of the integral field unit (IFU) fiber bundle. Replacing the DTU signal with the optical guider's 30Hz error signal stabilizes the pointing to the level of just a few arcseconds RMS. A schematic of one of the three FIREBALL control loops is shown in Figure 2.

2.1 Optical Guider

The FIREBALL optical guider is mounted in a pressure-canister behind a dichroic beam-splitter near the focal plane of the telescope (Figure 3). The reflected UV light is focused onto the IFU fiber bundle. The transmitted visible light is focused by a custom made focal ratio reducing triplet lens onto the detector of a commercial camera. The optics are aligned so that the field of view of the spectrograph falls near the center of the field of view of the guider camera. Additionally, the IFU and the guider are confocal at visible wavelenghts, making the optical guider the principal tool for focusing the telescope in the UV, as the UV channel is achromatic. The focal ratio reducing triplet has a nearly distortion-free performance, introducing only some coma near the edges of the image. The FIREBALL optical guider camera is a QImaging Retiga EXi that had previously been used by the HEFT telescope.[10] It is a 1360 × 1036 frame-buffer CCD with 6.45 μm square pixels that can be read out at 20MHz in 8-bit mode. This corresponds to 9Hz readout for the full chip. It is possible to use this camera in region-of-interest (ROI) mode; FIREBALL does so, reading out 200×200 pixel subarrays at 30Hz. The camera is connected via a Firewire cable to a PC104 computer stack running Ubuntu GNU/Linux.[11] The data from the camera is processed and displayed using the SVGALib[12] suite of libraries. The computer is commanded from the ground via a serial link. The operator can designate tracking points and stars, alter the video display, or

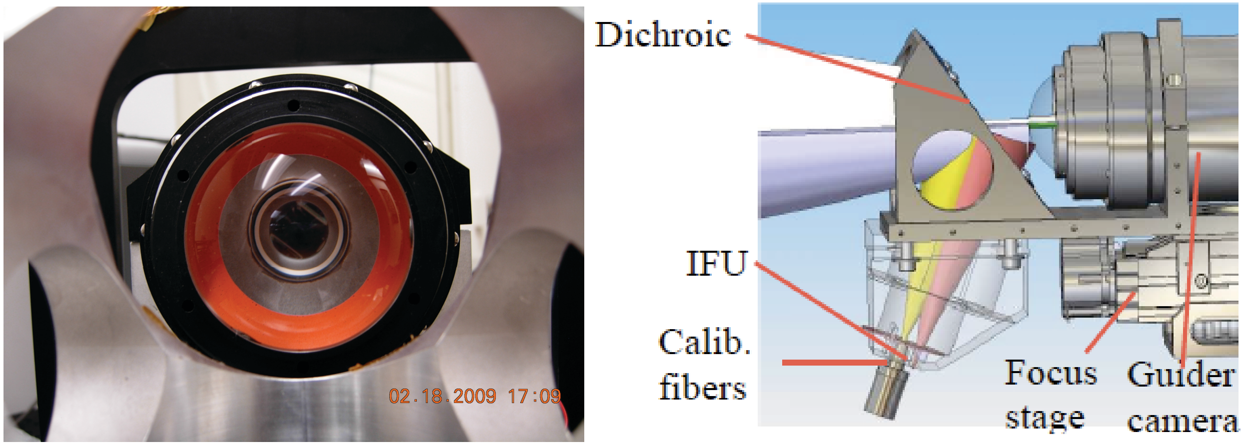

Figure 3. A face-on view of the FIREBALL guider camera (left panel). The CCD can be seen through the custom focal-ratio reducing lens. The right panel shows a zoomed-in view of the FIREBALL focal plane. The UV component of the telescope beam, entering from the left in the image, is reflected into the IFU fiber bundle. The visible light is transmitted and collected by the guider camera.

switch between the two optical sensors. The guider CCD axes are aligned with the gondola elevation and cross-elevation directions. The computer processes images from the camera, and performs a quick source extraction and offset calculation. It then reports these offset errors to the guidance control loop as proportional analog voltages. Housekeeping and pointing information is returned to the ground via another serial link(see Rahman et al.[5]). This data includes instantaneous offset information for every guider exposure, locations of multiple stars within the field of view, and general status information. The guider display is relayed to the ground using an NTSC video transmitter. The guider computer also interfaces with the detector computer, sending frame timing information to the latter to tag the incoming detector events with data that is later used to reconstruct the pointing. The guider can operate in one of two modes. The first makes use of the full CCD, giving a large field of view, but only delivering offset errors at 9Hz. The other makes use of the region of interest capabilities of the camera, giving a smaller field of view but operating at 30Hz. The two modes are compared in Table 1; the guider displays for the two modes are shown in Figures 4 and 5.

	Full Chip Mode	ROI Mode
Purpose	Field recognition Pointing correction	Fine guidance Telescope focus
Field of view	28'×22'	4'×4'
Resolution	1.25"/pixel	
Error update frequency	9Hz	30Hz
Exposure time (typical)	100ms	30ms
Image storage	Every 10th	Every 5th
Additional data stored	positions of 10 brightest stars	guide star RMS diameter

Table 1. Comparison of the two principal modes of the FIREBALL optical guider.

3. IN-FLIGHT PROCEDURE AND POST-FLIGHT RECONSTRUCTION

A typical observation begins with designating and uploading science target coordinates to the gondola control electronics. The pivot azimuth and siderostat elevation are adjusted to point at the relevant region of sky, and the DTU star-tracker obtains a solution and stabilizes pointing. A suitable tracking star is selected from the optical

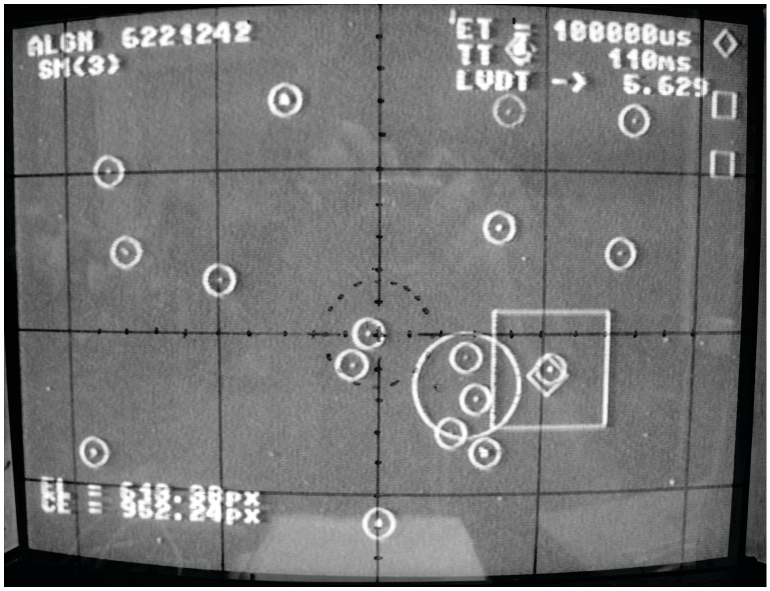

Figure 4. A photograph of a full-CCD video frame sent back to the ground during flight. The stars that the software has detected are encircled. The large circle near the center is the location of the FIREBALL fiber bundle. The diamond that contains a star marks the current location of the tracking point.

Figure 5. A photograph of a ROI frame. The box in the top left contains the full ROI, the cartoon of the full CCD in the bottom left shows the location of this region on the chip, and the box at the bottom right shows a blow-up of the star being tracked. Data, including GPS location, spot size and x-y offsets of the star from the tracking point, are also displayed.

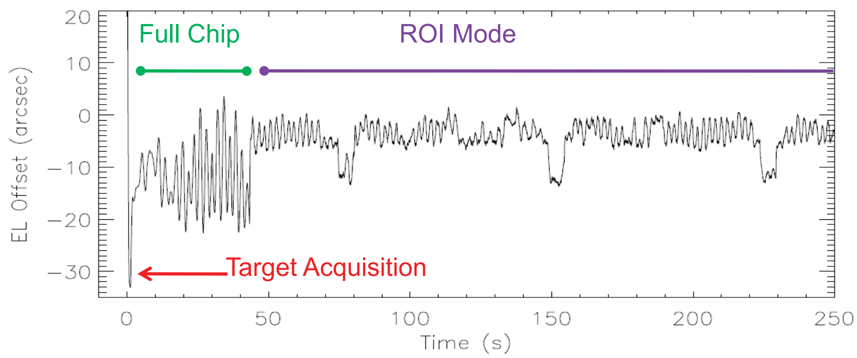

Figure 6. A sample tracking curve from the FIREBALL flight. The curve shows the elevation axis offset (in arcseconds) between the star being used for guidance and the guider CCD pixel designated as the tracking point. There is a short (about 2s) period of target acquisition where the pointing is transitioned from the DTU ASC tracking to guider tracking, followed by about 40s of guider operating in full-CCD mode where the pointing is verified and adjusted slightly. The guidance is then switched into the region of interest mode where the error signals are updated at 30Hz. The RMS variation in the residuals in the ROI mode is about 3". The periodic troughs on ∼75s period are due to the change in direction of the motion of the pivot.

guider field of view, and a command is issued for the guider to take control of the pointing. Once the starfield is confirmed, a new tracking point is designated for this guide star that places the science target onto the IFU fiber bundle. When the new tracking coordinates are established, the guider is switched from the 9Hz full chip mode to the 30Hz ROI mode. To ensure a more uniform sampling of the target region, a dither is performed. Periodically the guider is switched back to the full-CCD mode to confirm pointing, adjust if necessary, and provide reference images for post-processing. During the 6.5 hours of science observations, FIREBALL targeted 3 fields of scientific interest and two calibration stars. The instrument tracked on 9 different stars ranging in V magnitude from 8 to 12. Although fainter stars can be seen with the guider CCD, the short exposure times and the field motions due to the balloon environment and to dithering and pointing adjustment make reliable and consistent centroiding of these dimmer stars impossible.

Post-flight aspect reconstruction begins with finding an astrometric WCS solution to as many of the stored full-CCD frames from the flight as possible, using the Astrometry.net software.[13] These WCS solutions are then transformed for all ROI frames. This is possible as the celestial coordinates of the star being used for tracking and its location on the guider CCD are known for each frame. An existing WCS solution from a full frame that uses the same star for tracking is then translated to match the change in the trackstar location and corrected for any field rotation that may have occurred. (See Figure 6 for a sample tracking curve). The gondola does not remain stationary during an observation; there are azimuthal, pendulum and other disturbances (Figure 7) present. Compensating for these motions with the pivot and siderostat motion induces an additional field rotation (Figure 8) in addition to the already existing astronomical field rotation present due to FIREBALL being, effectively, an alt-az mount telescope. This field rotation is corrected for either by using the measured value from a pair of stars, if available, or by relying on computed values from the gondola housekeeping data. Once the WCS coordinates for the duration of an observation have been obtained, the location of the IFU fibers is known and the data collected by them can be tagged with celestial coordinates.

4. CONCLUSIONS

During the flight, the FIREBALL telescope achieved pointing stability of a little over 3" RMS in the elevation direction and 8" RMS in the cross-elevation or azimuthal direction. That is mainly due to the siderostat gimbal mount, with the mirror installed weighing close to the limit of the operating range of the mechanism responsible for the cross-elevation motion. This caused less stable motion in the azimuthal axis than in the elevation axis. The combination of the 30Hz guider offset signal with the very fine time-resolution of the photon-counting FIREBALL microchannel plate detectors allowed for the pointing accuracy to be improved with post-flight

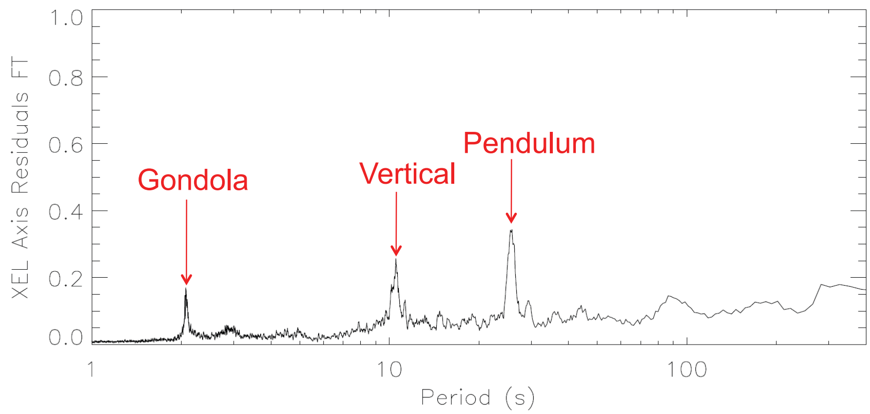

Figure 7. A fast Fourier transform of a cross-elevation axis residual offset signal. The highlighted peaks correspond to various oscillation frequencies within the system. The shortest period oscillation is a normal mode of the gondola around its center of mass. Also present are a vertical elastic mode of the balloon-gondola train, and pendulum motion of the payload suspended from the balloon. There are also altitude-pressure oscillations of the balloon that have a period near 300 s. The time interval for which this fourier transform was calculated was not long enough to show this signal clearly.

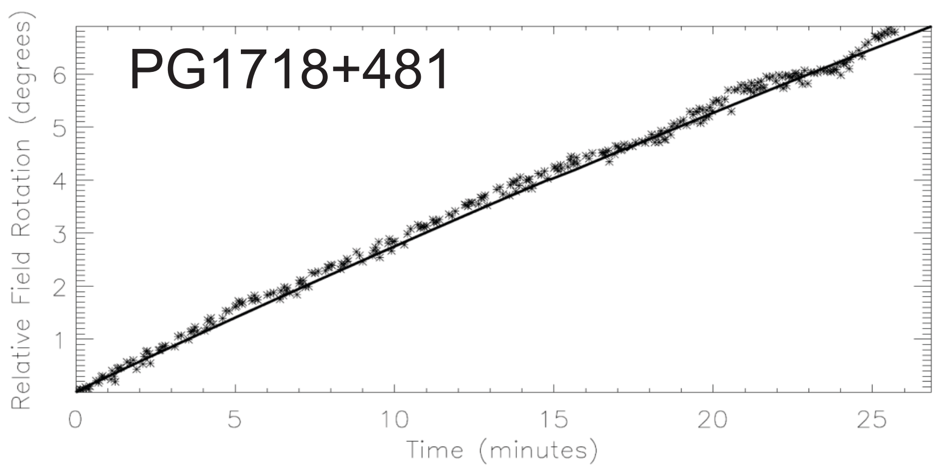

Figure 8. A sample field rotation curve from flight. The solid line shows the astronomical field rotation; the scattered points are the measured field rotation using two stars that were present in the guider field of view during the observation. The deviation can also be calculated from the on-board instrument data for cases when no multiple objects are present in the guider images.

reconstruction. The estimated error for the calculations is 3". Centroiding errors are on the order of 1", field rotation inaccuracies add another 2", with additional systematics contributing no more than an extra 2" . A reconstruction of one of our targets is shown in Figure 9.

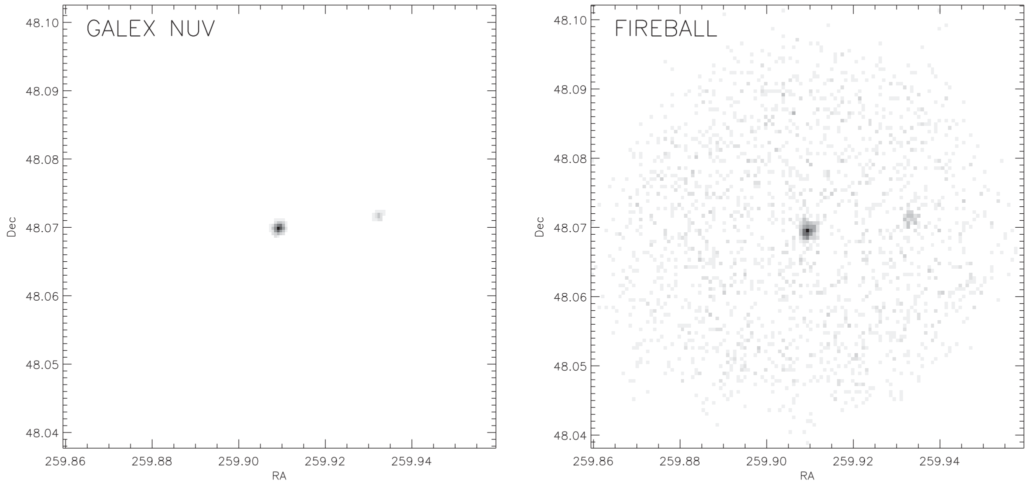

Figure 9. Comparison of the reconstruction of the region around PG1718+481. The left panel shows a processed GALEX AIS image, the right panel the FIREBALL data collapsed in the wavelength direction and background-subtracted. The FWHM of the resultant spots is about 10", and their location is accurate to 1.5" as compared with the GALEX data.

FIREBALL is being modified for another campaign. The cross-elevation motor will be replaced with a more powerful actuator that should improve the in-flight pointing stability in that axis. This change will be key for the anticipated replacement of the microchannel plate detector with δ-doped L^3 CCDs that would need to integrate signal on few-hundred second timescales.

ACKNOWLEDGMENTS

The material is based upon work supported by NASA under award No. NNX08AO39G. The FIREBALL collaboration also acknowledges support from CNES, LAM and CNRS.

REFERENCES

[1] Faucher-Giguère, C., Lidz, A., and Hernquist, L., "Numerical Simulations Unravel the Cosmic Web," *Science* **319**, 52– (Jan. 2008).

[2] Furlanetto, S. R., Schaye, J., Springel, V., and Hernquist, L., "Mapping the Cosmic Web with Lyα Emission," *ApJ Letters* **599**, L1–L4 (Dec. 2003).

[3] Martin, D. C., Milliard, B., Schiminovich, D., Evrard, J., and the FIREBALL collaboration, "FIREBALL: An overview of the Faint Intergalactic Redshifted Emission Balloon," **7792**(4) (2010).

[4] Tuttle, S. E., Schiminovich, D., Grange, R., Rahman, S., Matuszewski, M., Milliard, B., Deharveng, J.-M., and Martin, D. C., "FIREBALL: The first ultraviolet fiber fed spectrograph," in [*Proc. SPIE*], **7732**(78) (2010).

[5] Rahman, S., Matuszewski, M., Tuttle, S. E., Milliard, B., Shiminovich, D., Martin, D. C., Frank, S., Evrard, J., Vibert, D., and Mirc, F., "FIREALL: Detector, data acquisition and reduction," in [*Proc. SPIE*], **7732**(79) (2010).

[6] Milliard, B., Donas, J., Laget, M., and Huguenin, D., "The balloon-borne 40-cm UV-(200 nm) imaging telescope FOCA: results and perspective.," in [*ESA Special Publication*], E. J. Rolfe, ed., *ESA Special Publication* **183**, 253–257 (Mar. 1994).

[7] Serra, G., Giard, M., Bouchou, F., Dupac, X., Gabarrot, F., Meny, C., Ristorcelli, I., Lamarre, J. M., Bernard, J. P., Pajot, F., Stepnick, B., and Torre, J. P., "PRONAOS : a two meter submillimeter balloon borne telescope," *Advances in Space Research* **30**, 1297–1305 (2002).

[8] Huguenin, D., "Design and performance of stratospheric balloon-borne platforms for infrared astrophysical observations," *Infrared Physics and Technology* **35**, 195–202 (Mar. 1994).

[9] Joergensen, J. L. and Pickles, A. J., "Fast and robust pointing and tracking using a second-generation star tracker," in [*Society of Photo-Optical Instrumentation Engineers (SPIE) Conference Series*], H. Lewis, ed., *Presented at the Society of Photo-Optical Instrumentation Engineers (SPIE) Conference* **3351**, 51–61 (May 1998).

[10] Chonko, J. C., *Development and first flight of the high energy focusing telescope and analysis of spectral features in the isolated neutron star 1E1207.4-5209*, PhD thesis, Columbia University, United States – New York (2006).

[11] "Ubuntu GNU/Linux." `http://www.ubuntu.com/`.

[12] "SVGAlib." `http://www.svgalib.org/`.

[13] Lang, D., Hogg, D. W., Mierle, K., Blanton, M., and Roweis, S., "Astrometry.net: Blind Astrometric Calibration of Arbitrary Astronomical Images," *Astronomical Journal* **139**, 1782–1800 (May 2010).